

ELEMENTS OF LASER DEVICES

PACS numbers: 85.70.Sq; 42.65.An; 42.25.Ja
DOI: 10.1070/QE2013v043n10ABEH015201

Influence of cubic nonlinearity on compensation of thermally induced polarisation distortions in Faraday isolators

M.S. Kuzmina, E.A. Khazanov

Abstract. **The problem on laser radiation propagation in a birefringent medium is solved with the allowance made for thermally induced linear birefringence under the conditions of cubic nonlinearity. It is shown that at high average and peak radiation powers the degree of isolation in a Faraday isolator noticeably reduces due to the cubic nonlinearity: by more than an order of magnitude when the *B*-integral is equal to unity. This effect is substantial for pulses with the energy of 0.2–3 J, duration of 10 ps to 4 ns and pulse repetition rate of 0.2–40 kHz.**

Keywords: *laser systems with high peak and high average powers, thermally induced birefringence, cubic nonlinearity, polarisation distortions.*

1. Introduction

One of promising directions in laser physics evolution is the development of laser systems simultaneously possessing a high average power and a high peak power. In designing such lasers, most significant are both thermal effects, which limit the average power, and parasitic nonlinear-optical effects, which limit the peak power. The parameters of such lasers vary in a wide range: from femto- and picosecond lasers with the pulse energy of a fraction of joule and a pulse repetition rate ~1 kHz to nanosecond neodymium glass lasers with the energy of several hundred joules and a pulse repetition rate equal to tenth or hundredth of Hz; therefore, the range of applications for such lasers is rather wide.

Actual are investigations of a combined (simultaneous) action of thermal and nonlinear-optical effects. In particular, interesting is propagation of light through a medium with the birefringence induced by two simultaneous effects: thermoelastic stresses and cubical nonlinearity. The contributions of these effects are not additive because thermally induced birefringence is independent of intensity or laser polarisation, whereas the anisotropy induced by cubical nonlinearity depends on intensity and polarisation. A Faraday isolator being a key element in many laser systems refers to the optical elements for which consequences of the mutual influence of cubical nonlinearity and thermal effects may become critical.

Thermal effects arising in a Faraday isolator are caused by the relatively high absorption of laser radiation in its magnetically active element 10^{-3} cm^{-1}. The absorption of radiation causes a non-uniform temperature cross-section distribution and leads to formation of a thermal lens, a nonuniform distribution of the rotation angle of the polarisation plane, and linear birefringence caused by mechanical stresses due to a temperature gradient (the photo-elastic effect). The thermal lens produced does not change the polarisation state of laser radiation and, hence, does not affect the isolation properties of the Faraday isolator. According to [1, 2], the most important contribution into the reducing of isolation is made by the photo-elastic effect, whereas the effect of the non-uniform distribution of the rotation angle of polarisation plane can be neglected. Hence, in the present work, by the thermal self-action is meant exclusively the photoelastic effect, which changes not only the phase difference of eigen polarisations but also the polarisations themselves that in this case become elliptical. Ellipticity, ellipse axis orientation and phase difference are functions of transverse coordinates. All these factors result in the depolarisation of radiation, which has a negative consequence in that the non-isolation (the parameter inverse to the degree of isolation) of Faraday isolators becomes distinct from zero. By depolarised radiation is meant radiation with the polarisation constant in time but varying from point to point in a transverse cross section. Hence, depolarisation is the transfer from polarised radiation to depolarised.

Presently, there are several papers devoted to the problem of compensation of thermally induced distortions in a Faraday isolator [1–5], and so we will be interested in how the cubic nonlinearity affects the already known methods for withstanding the negative thermal effect mentioned above.

Manifestation of cubic nonlinearity in a magnetically active element of a Faraday rotator, which possesses, with respect to laser glass, a relatively small optical thickness, is explained by the greater value of the medium nonlinear characteristic: $\gamma_{nl} = 7.2\times10^{-7}$ (glass magnetically active element) and 17×10^{-7} GW^{-1} cm^2 [crystal of terbium–gallium garnet (TGG)], where γ_{nl} determines the dependence of the refractive index on intensity $n(I) = n_0 + \gamma_{nl}I$. Cubic nonlinearity is also measured by using the *B*-integral, i.e., the nonlinear phase incursion in a medium of length L:

$$B(r) = \frac{2\pi}{\lambda}\gamma_{nl}\int_0^L I(r,z)\,\mathrm{d}z,$$

where λ is the light wavelength in vacuum and r is the radius in the cylindrical system of coordinates. By the effect caused by cubic nonlinearity will be meant the polarisation effect related with an origin of field-induced anisotropy. The difference in the refractive indices arising in this case for the circularly polarised waves results in a turn of the polarisation ellipse [6, 7].

M.S. Kuzmina, E.A. Khazanov Institute of Applied Physics, Russian Academy of Sciences, ul. Ul'yanova 46, 603950 Nizhnii Novgorod, Russia; e-mail: kmsnn@mail.ru, khazanov@appl.sci-nnov.ru

Received 16 April 2013; revision received 27 June 2013
Kvantovaya Elektronika **43** (10) 936–942 (2013)
Translated by N.A. Raspopov

Thus, both cubic nonlinearity and thermally induced birefringence introduce polarisation distortions in the laser beam (depolarisation arises). Hence, in laser systems with high average and peak powers, the problem arises on considering changes in polarisation of laser radiation in the medium with circular birefringence (Faraday effect) and with two parasitic effects, namely, thermally induced linear birefringence and nonlinear circular birefringence. The problem is a continuation of studies [8] concerning the influence of cubic nonlinearity on the efficiency of compensating thermally induced distortions in glass active elements. There are two substantial differences between these problems. First, the active element problem does not consider circular birefringence, which principally should be taken into account in the case of a Faraday isolator. Second, in compensating for thermally induced birefringence in active elements, the integral residual depolarisation of ~1% is admissible. In the case of the Faraday isolator, the non-isolation is a very important parameter, which in modern devices should not exceed 0.1%. This is why at equal *B*-integrals the influence of cubic nonlinearity on the non-isolation of the Faraday isolator is more substantial than its influence on the accuracy of compensating for thermally induced distortions in laser active elements. Nevertheless, the heat release and, hence, the thermally induced birefringence in isolators is lower than in active elements.

In the present work, we study propagation of laser radiation in a magnetically active medium possessing thermally induced linear birefringence and cubic nonlinearity. The influence of cubic nonlinearity is studied on characteristics of modern widely used schemes for compensating for thermally induced birefringence in Faraday isolators with glass (MOG 10) and crystal (TGG crystal) magnetically active elements.

2. Propagation of laser radiation in an absorbing magnetically active element with cubic nonlinearity

Consider the case of a magnetically active medium and choose the propagation direction of laser radiation along z axis. Then, the vector of the electric field intensity $\boldsymbol{E}$ has projections to axes x and y. For the magnetically active medium we choose the two possible types: magnetically active glass (MOG 10) and TGG crystal with orientation [001]. In both media, the cubic nonlinearity is assumed isotropic. For a TGG crystal this is an approximation which usually holds true in isotropic crystals (authors have no data on the values for off-diagonal components of the nonlinear susceptibility tensor).

By neglecting diffraction, one may write the stationary system of differential equations for components of the vector $\boldsymbol{E}$ in the case of radiation propagation in the nonlinear medium possessing linear and circular birefringence:

$$\frac{\partial E_x}{\partial z} = \frac{\mathrm{i}6\pi k_0}{n_0}\chi_{xxxx}\left[|E_x|^2E_x + \frac{1}{3}(2E_x|E_y|^2 + E_x^*E_y^2)\right]$$

$$-\frac{\mathrm{i}}{2}\frac{\partial\delta_{\mathrm{lin}}}{\partial z}\cos(2\Psi)E_x - \left[\frac{\partial\delta_{\mathrm{circ}}}{\partial z} + \mathrm{i}\frac{\partial\delta_{\mathrm{lin}}}{\partial z}\sin(2\Psi)\right]E_y, \quad (1)$$

$$\frac{\partial E_y}{\partial z} = \frac{\mathrm{i}6\pi k_0}{n_0}\chi_{xxxx}\left[|E_y|^2E_y + \frac{1}{3}(2E_y|E_x|^2 + E_y^*E_x^2)\right]$$

$$+\frac{\mathrm{i}}{2}\frac{\partial\delta_{\mathrm{lin}}}{\partial z}\cos(2\Psi)E_y + \left[\frac{\partial\delta_{\mathrm{circ}}}{\partial z} - \mathrm{i}\frac{\partial\delta_{\mathrm{lin}}}{\partial z}\sin(2\Psi)\right]E_x,$$

where $k_0 = 2\pi/\lambda$; χ_{xxxx} is the diagonal component of the 4th rank nonlinear susceptibility tensor; δ_{circ} and δ_{lin} are the phase differences for purely circular (without linear) and purely linear (without circular) birefringence, respectively; and Ψ is the inclination angle of eigen polarisation relative to the x axis for a purely linear birefringence (Fig. 1). Note that the rotation angle of laser radiation polarisation caused by the Faraday rotator is $\Phi = \delta_{\mathrm{circ}}(L)/2$. Despite the fact that the considered thermal and nonlinear effects are caused by the self-action of laser radiation, their common contribution into (1) can be described as a sum of the corresponding summands due to the difference in the transition times. Indeed, the cubic nonlinearity is characterised by a short relaxation time (10^{-15}–10^{-16} s) [9] and becomes actual only for the pulsed radiation with a high power and a short duration (1 ns and less). The response time of a medium to the thermal action is much longer than the cubic nonlinearity transition time. Hence, the considered thermal effect of self-action is revealed in the medium after the transition process finishes and a stationary regime is established. This is why the cubic nonlinearity for a single short pulse appears instantaneously on the background of the stationary thermal action.

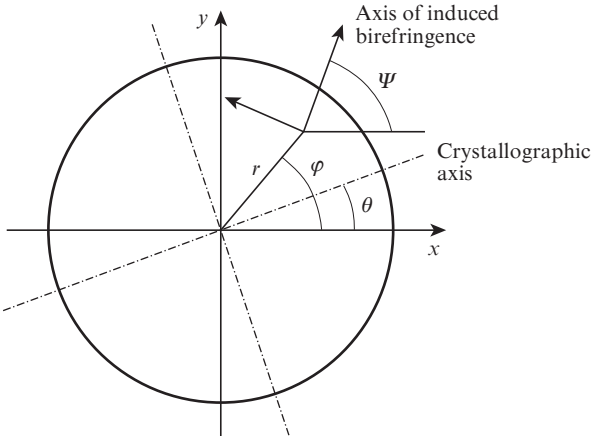

Figure 1. Cross section of a magnetically active crystal: r, φ are the polar coordinates; θ is the inclination angle of the crystallographic axis; Ψ is the inclination angle of eigen polarisation at purely linear birefringence (in the case of glass magnetically active material $\Psi = \varphi$).

Assume that the radiation after passing the first transit across the Faraday isolator (at point A in Fig. 2) has a Gaussian transverse intensity distribution, and the radiation polarisation is linear and directed along the x axis:

$$\boldsymbol{E}_0(r) = \boldsymbol{x}_0 e_0 \exp\left(-\frac{r^2}{2r_0^2}\right),$$

where x_0 is a unit vector along the x axis. Then, for an infinitely long cylindrical magnetically active element one can employ the expressions [3, 10, 11]:

$$\delta_{\mathrm{lin}}(r,\varphi) = 2p\left[r_0^2\frac{1-\exp(-r^2/r_0^2)}{r^2} - 1\right]$$

$$\times\left[\cos^2(2\varphi - 2\theta) + \xi^2\sin^2(2\varphi - 2\theta)\right]^{1/2}, \quad (2)$$

$$\tan(2\Psi - 2\theta) = \xi\tan(2\varphi - 2\theta), \quad (3)$$

where θ is the inclination angle of the crystallographic axis (Fig. 1);

$$p = \frac{L}{\lambda}\frac{\alpha Q}{\kappa}P;\ Q = \left(\frac{1}{L}\frac{\mathrm{d}L}{\mathrm{d}T}\right)\frac{n_0^3}{4}\frac{1+\nu}{1-\nu}(p_{11}-p_{12});$$
$$\xi = \frac{2p_{44}}{p_{11}-p_{12}}; \tag{4}$$

ν, κ, α, p_{ij} are the Poisson coefficient, thermal conduction, absorption coefficient, and photoelasticity coefficients of magnetically active medium, respectively; $P = \pi r_0^2 I$ is the power of laser radiation; T is the temperature of magnetically active element; and $\xi = 2.2$ for TGG crystal [10] and $\xi = 1$ for MOG.

At a prescribed parameter ξ the non-isolation of Faraday isolator is completely determined by the normalised power of heat release p and by the B-integral. In the calculations we used $Q = 17\times10^{-7}$ K^{-1}, $k = 5\times10^{-2}$ W K^{-1} cm^{-1}, $\alpha = 7\times10^{-4}$ cm^{-1} [5], $L = 2$ cm, $\chi_{xxxx} = 1.66\times10^{-13}$ esu [12,13] for TGG crystal and $Q = 5\times10^{-7}$ K^{-1} [14], $k = 0.5\times10^{-2}$ W K^{-1} cm^{-1} [14], $\alpha = 10^{-3}$ cm^{-1} [15], $L = 3$ cm, $\chi_{xxxx} = 5.67\times10^{-14}$ esu [16] for the magnetically active glass.

3. Basic schemes of the Faraday isolator

Consider the basic schemes of the Faraday isolator presented in Fig. 2: a traditional scheme and schemes with internal [3] and external [5] compensation of thermally induced polarisation distortions.

In all the schemes without thermal and nonlinear effects, after a first passage (from left to right) through the Faraday isolator the beam preserves the horizontal polarisation (in the plane of the figure) and passes through polariser (*4*); in the backward transit the beam changes its polarisation to vertical (normal to the figure plane) and is reflected by polariser (*1*). The linear birefringence caused by the photoelastic effect and the circular birefringence due to the cubic nonlinearity result in the radiation which, after a reverse transit, has the horizontal polarisation and passes through polariser (*1*) (the non-isolation radiation). The non-isolation of a Faraday isolator at certain point we will define as the part of radiation intensity with the horizontal polarisation:

$$\Gamma(r,\varphi) = \frac{|\boldsymbol{E}\boldsymbol{E}_0|^2}{|\boldsymbol{E}_0|^2|\boldsymbol{E}|^2}, \tag{5}$$

where $\boldsymbol{E}$ is the field in the reverse transit through the Faraday isolator (point B in Fig. 2).

Most interesting is the non-isolation integral over the beam cross section

$$\gamma = \left[\int_0^{2\pi}\mathrm{d}\varphi\int_0^{\infty}\Gamma(r,\varphi)\exp\left(-\frac{r^2}{r_0^2}\right)r\,\mathrm{d}r\right]$$
$$\times\left[\int_0^{2\pi}\mathrm{d}\varphi\int_0^{\infty}\exp\left(-\frac{r^2}{r_0^2}\right)r\,\mathrm{d}r\right]^{-1}. \tag{6}$$

Here we assume that the light diameter of the Faraday isolator is such that aperture losses may be neglected and one may integrate in (6) over polar radius r to infinity.

The scheme with internal compensation of thermally induced distortions (Fig. 2b) comprises, arranged in-line along the optical axis, polarisers (*1*) and (*4*), Faraday rotator of polarisation plane (*5*) and half-wavelength plate (*2*). The Faraday rotator comprises two magnetically optical elements placed in a magnet system, each rotating the polarisation plane by 22.5°. Between the magnetically active elements there is the reciprocal optical element in the form of quartz plate which rotates the polarisation plane by the angle $\beta_R = 67.5°$.

The scheme with external compensation of polarisation distortions (Fig. 2c) comprises, arranged in-line along the optical axis, polarisers (*1*) and (*4*), Faraday rotator (*3*), which rotates the polarisation plane by the angle of 45°, compensating element (*7*), reciprocal polarisation rotator (*6*), which rotates the polarisation plane of passing radiation by the angle of 67.5°, and half-wavelength plate (*2*). The material of the compensating element may differ from that of magnetically active element (*3*), and the parameters of reciprocal polarisation rotator (*6*) and element (*7*) are calculated by using the parameters of element (*3*) and thermo-optical constants for the material of the compensating element. In the present work we consider the case of using a TGG crystal as the compensating element.

In the schemes given in Figs 2a and 2b, glass and TGG crystal will be considered as magnetically active media; in the last scheme (Fig. 2c) only TGG crystal will be considered. In Table 1, the values are given, which are optimal from the viewpoint of least integral non-isolation γ_{min}, for the parameters β_R, β_L, θ_{opt} and p_2/p_1 (the ratio of normalised powers of heat release in the two magnetically active elements for the schemes in Figs 2b and2c) for all three schemes at $B = 0$ and $\theta_1 = \theta_2 = \theta_{opt}$ (for TGG crystal).

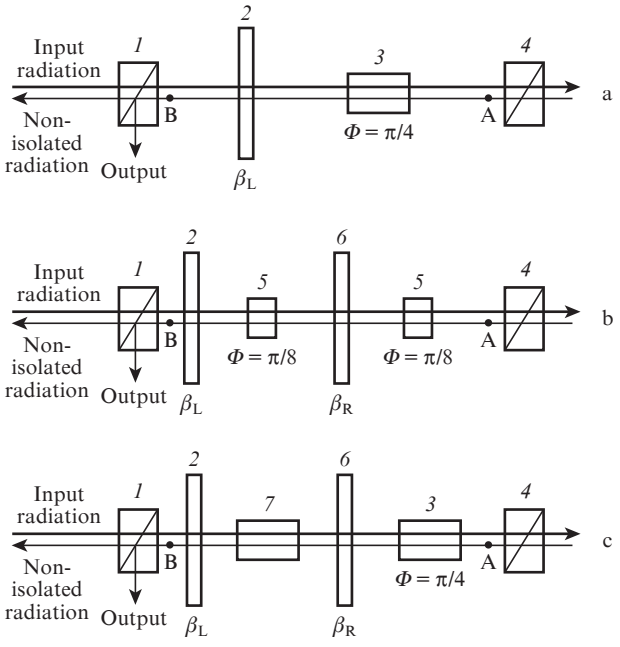

Figure 2. Schematic diagrams of (a) traditional Faraday isolator, Faraday isolators with (b) internal [3] and (c) external [5] compensation: (*1*,*4*) polarisers; (*2*) plate $\lambda/2$ with the inclination angle of optical axis relative to the x axis equal to β_L; (*3*) Faraday rotator 45°; (*5*) Faraday rotator 22.5°; (*6*) reciprocal rotator of polarisation plane; (*7*) compensating optical element.

4. Influence of cubic nonlinearity on the non-isolation of the Faraday isolator

Figures 3a and 3c show the integral non-isolation γ versus normalised power of heat release p at various values of the

Table 1. Characteristics for three schemes of Faraday isolators at $B = 0$ and $\theta_1 = \theta_2 = \theta_{opt}$ [3, 5].

Scheme	θ_{opt} (TGG)/rad	β_R/rad	β_L/rad	p_2/p_1	γ_{min} at $\delta_{lin} \ll 1$
Traditional (Fig. 2a)	$-\pi/8$	–	$-\pi/8$	–	$1.4\times10^{-2}p^2$
With internal compensation (Fig. 2b)	$\pi/16$	$3\pi/8$	$\pi/8-\beta_R/2$	1	$0.4\times10^{-5}(\xi^4 + {}^2/_3\xi^2 + 1)p^4$
With external compensation (Fig. 2c)	$\pi/16$	$3\pi/8$	$\pi/8-\beta_R/2$	$8^{1/2}/\pi$	$5.3\times10^{-5}(\xi^4 + {}^2/_3\xi^2 + 1)p^4$

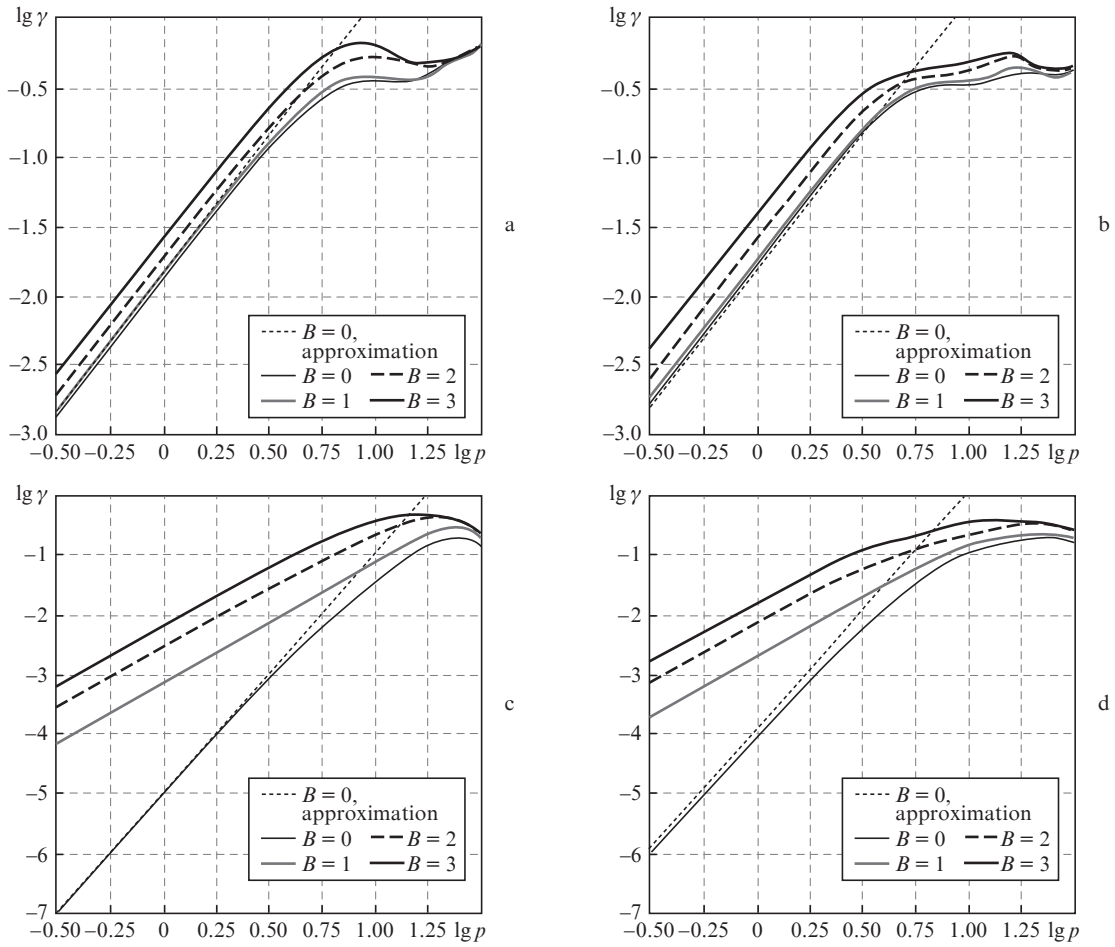

Figure 3. Integral non-isolation γ vs. normalised heat release power in magnetically active element p in (a, b) the traditional scheme (Fig. 2a) and in (c, d) the scheme with internal compensation (Fig. 2b) with employment of (a, c) magnetically active glass and (b, d) TGG crystal. Dotted curves refer to the dependences derived by the formulae from Table 1 at $B = 0$ in the approximation $\delta_{lin} \ll 1$, the rest curves are numerical solutions of system (1).

B-integral for the traditional scheme (Fig. 2a) and for the scheme with internal compensation (Fig. 2b) and glass used as a magnetically active material. The same dependences for a TGG crystal are shown in Figs 3b and 3d.

Note that the values of the B-integral and the normalised power of heat release presented in the work correspond to the values in the Faraday rotator, which turns the polarisation plane by the angle of $\pi/4$ at the length equal to L. In other words, the sum of values B (or p) in the two elements of the Faraday rotator of length $L/2$ each in the scheme with internal compensation equals to the value of B (or p) in one element for the traditional scheme and for the scheme with external compensation of depolarisation. In calculations for the schemes with internal and external compensation of depolarisation, the influence of the cubic nonlinearity was taken into account in polarisation rotator (*6*) and in compensating element (*7*).

At $B = 0$ the difference between employment of magnetically active glass and TGG crystal is insufficient. At increasing B, the efficiency of compensation of thermally induced depolarisation falls. In the traditional scheme, the character of dependence $\gamma(p)$ does not change (Figs 3a and 3b). In the scheme with internal compensation (Figs 3c and 3d), in addition to a noticeable increase in non-isolation, the character of its dependence on the power of heat release also changes: γ becomes proportional not to p^4 but to p^2. Such a strong (as compared to the traditional scheme) effect can be explained as follows. The birefringence caused by cubic nonlinearity is proportional to the difference of intensities of two circularly polarised components of radiation [9]. Such nonlinear birefringence only occurs at nonzero ellipticity of radiation polarisation and is absent in the case of a linearly polarised radiation. Hence, without thermal effects ($p = 0$) the nonlinear effect is also absent ($\gamma = 0$) because the polarisation of radiation is definitely linear in this case. If $p \neq 0$, then there are nonlinear distortions of polarisation, which, however, are small as compared to thermal distortions, because these are second-order

effects. In the compensating schemes (Figs 2b and 2c) thermal effects are well suppressed; hence, the influence of cubic nonlinearity becomes noticeable.

Similar investigation of the cubic nonlinearity effect on the compensation of thermally induced depolarisation in the case of two identical active glass elements and 90-degree rotator of the polarisation plane placed between them was conducted in [8]. In the present work it was established that at the output of one of these elements the intensity distribution of the depolarised component weakly depends on the value of the B-integral. In the scheme with the 90-degree rotator of the polarisation plane the cubic nonlinearity has a noticeable effect: the integral degree of residual depolarisation in this scheme is proportional to B^2. This result is explained by the fact that the nonlinear birefringence violates the equality of the phase difference acquired by linear eigen polarisations of light passing through the two active elements that are identical from the viewpoint of thermally induced polarisation distortions.

The dependences of $\gamma(p)$ for the schemes with internal and external compensation of thermally induced distortions in the Faraday rotator in the case of the B-integral increasing from 0 to 3 are shown in Fig. 4 for the case of TGG crystal. Separate consideration of these schemes is explained by fact that they may be optimised from the viewpoint of least non-isolation for the case $B = 0$ by adjusting the orientations of crystallographic axes (optimal relation between θ_1 and θ_2) in two TGG crystals and by choosing parameters β_R, p_2/p_1 for each value of normalised power of heat release p (Figs 4b and 4d). For the scheme with internal compensation the optimal parameters are $\beta_R \approx 73.18°$, $p_2/p_1 \approx 0.964$, $\theta_1 \approx 20°$ and $\theta_2 \approx 15.3°$; whereas for the scheme with external compensation these parameters are $\beta_R \approx 73.5°$, $p_2/p_1 \approx 0.908$, $\theta_1 \approx 27.2°$ and $\theta_2 \approx 22.3°$ [5]. In the scheme with external compensation (Fig. 2c) and in the scheme shown in Fig. 2b, in addition to the increased non-isolation γ the latter becomes proportional not to p^4 but to p^2 at $B > 0$.

Figure 5 shows the dependences of the integral degree of depolarisation on the B-integral for the schemes corresponding to Figs 2b and 2c in the case of using TGG crystal at $p = 1$. Taking into account the quadratic dependence $\gamma(p)$ at $p < 3$ (Fig. 4), with the help of Fig. 5 one can easily determine γ for wide ranges of variation in parameters p and B. The calculations show that the increase in γ due to the cubic nonlinearity in these schemes is proportional to the product p^2B^2. In the general case, in the schemes shown in Figs 2b and 2c, the non-isolation is well described by the formula $\gamma(p, B) = ap^4 + bp^2B^2$, where factor a at standard parameters can be found by using the expressions for γ_{min} from Table 1 at $p = 1$. The values of a and b at optimal parameters for the considered schemes were obtained from a numerical solution of system of equations (1).

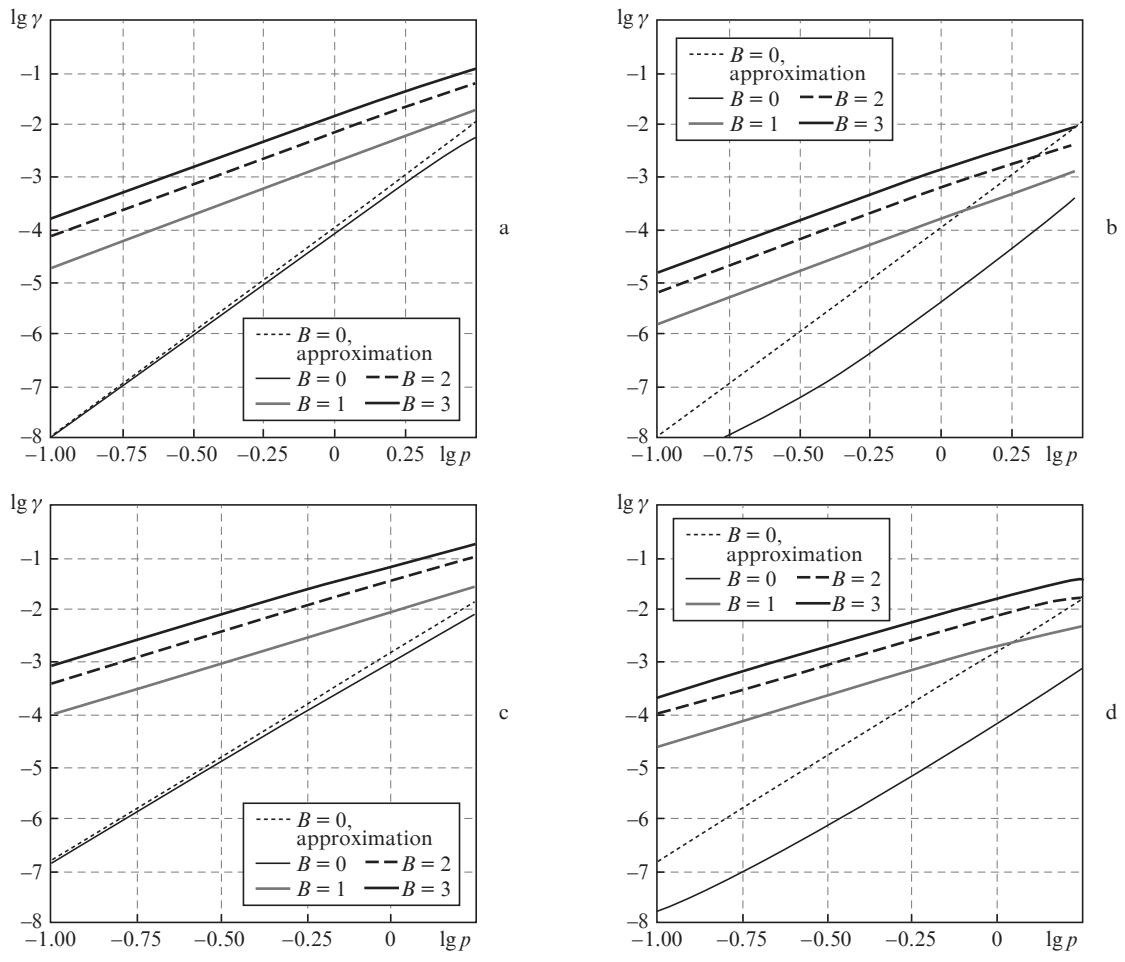

Figure 4. Integral non-isolation γ vs. the normalised power of heat release in a magnetically active element p for the schemes with (a, b) internal and (c, d) external compensation at (a, c) standard and (b, d) optimal values of parameters β_R, p_2/p_1, θ_1 and θ_2. Dotted curves denote dependences derived by the formulae from Table 1 at $B = 0$ in the approximation $\delta_{lin} \ll 1$, the rest curves are numerical solutions of system (1).

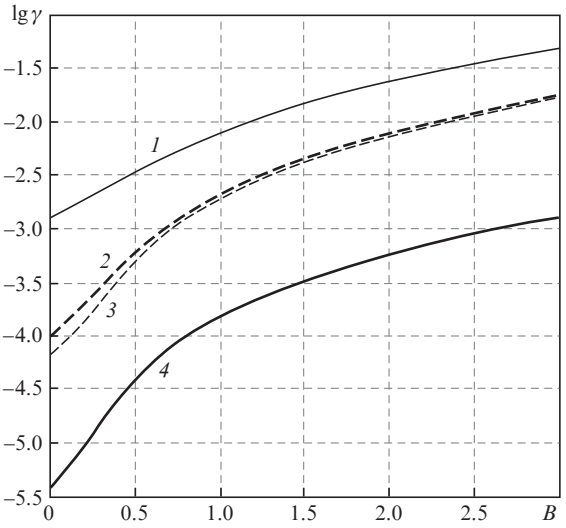

Figure 5. Integral non-isolation of Faraday isolator γ vs. the B-integral at $p = 1$ in the schemes with (*1*,*3*) external and (*2*,*4*) internal compensation in the case of the TGG crystal. Curves (*3*,*4*) correspond to the parameters optimised for $B = 0$.

Table 2. Coefficients a and b for the schemes with internal and external compensation at standard and optimal values of parameters β_R, p_2/p_1, θ_1 и θ_2 for the TGG crystal.

Scheme	Parameters	a	b
With internal compensation	Standard	1.1×10^{-4}	1.9×10^{-3}
	Optimal	4.0×10^{-6}	1.4×10^{-4}
With external compensation	Standard	1.5×10^{-3}	5.4×10^{-3}
	Optimal	6.6×10^{-5}	1.9×10^{-3}

Parameters a and b are given in Table 2 for a TGG crystal, the parameter of anisotropy of the latter is $\xi = 2.2$.

The value of γ plays an important role at $B = 0$, which depends on the efficiency of compensating polarisation distortions in the schemes from Figs 2b and 2c without cubical nonlinearity. Thus, if at $B = 0$ the scheme with internal compensation and optimal parameters has a minimal non-isolation, this will also be so if one takes into account the cubic nonlinearity. In the scheme with internal compensation and in the optimised scheme with external compensation the increase in B from zero to unity reduces the optical isolation from 42 to 27 dB, and for the optimised scheme with internal compensation – from 54 to 38 dB. Note that a TGG crystal is, generally speaking, an anisotropic medium with the cubic crystal lattice. The allowance made for off-diagonal components of nonlinear susceptibility tensor χ is liable to result in an increased non-isolation.

5. Discussion of results

As was shown above, the problem of influence of cubic nonlinearity on the non-isolation of the Faraday isolator is described by two dimensionless parameters, namely, the normalised power of heat release p and B-integral. One may estimate the dimensional parameters of laser radiation, at which its nonlinear self-action would increase the thermally induced non-isolation of the Faraday isolator with a TGG crystal used as a magnetically active element. We assume that the dimensionless parameters p and B vary within the following limits: $\lg p \in [-0.5, 0.5]$, and $B \in [0.5, 3]$. The reasons for considering such ranges for p and B values can be elucidated from Figs 4 and 5. At $\lg p < -0.5$ the value of thermally induced depolarisation is small even if its increase due to cubic nonlinearity is taken into account. Physically it is related with the fact that the polarisation of radiation remains close to linear, for which the rotation due to cubic nonlinearity is absent. If $\lg p > 0.5$ then, conversely, the Faraday isolator does not provide good isolation due to the thermal effect even at $B = 0$ and the influence of cubic nonlinearity in this case weakly worsens the situation (at $B < 3$). The lower limitation of B-integral values is determined by the fact that actually it is difficult to reach the non-isolation $\gamma < 10^{-4}$, and the upper limitation is explained by a starting development of beam self-focusing [6, 17–19].

Assume that the energy density of laser radiation corresponds to the optical breakdown threshold for a crystal (W_{th}). Consider a Gaussian beam with $r_0 = 0.3$ cm, which is typical for a Faraday isolator 1–2 cm in diameter. Define in these conditions the value of the B-integral and pulse energy ε_p as functions of pulse duration t_p assuming that at the pulse dura-

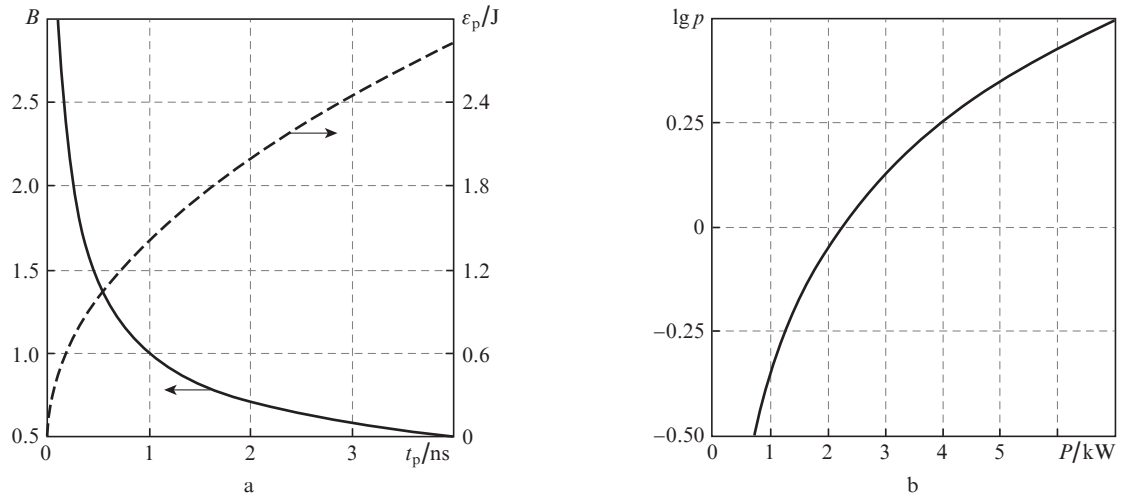

Figure 6. (a) Dependences of B and ε_p on pulse duration t_p for the TGG crystal of length $L = 2$ cm at $r_0 = 0.3$ cm, $W^*_{th} = 5$ J cm^{-2}, $t^*_p = 1$ ns, and (b) normalised power p vs. average power of laser radiation P.

tion $t_p^* = 1$ ns the threshold energy density is $W_{th} = 5$ J cm^{-2} [20]. In view of $I = \varepsilon_p/(\pi r_0^2 t_p)$ and $W_{th} \sim t_p^{1/2}$ [21–23] we obtain

$$B = k_0 \gamma_{nl} \frac{W_{th}^*}{\sqrt{t_p^* t_p}} L, \ \varepsilon_p = \pi r_0^2 W_{th}^* \left(\frac{t_p}{t_p^*}\right)^{1/2}. \quad (7)$$

Dependences (7) are shown in Fig. 6a, and the normalised power of heat release p is shown in Fig. 6b versus the average laser radiation power P derived from formulae (4) for a TGG crystal with the thermo-optical characteristics taken from Section 2 of the present work.

According to Fig. 6a, in a TGG crystal at the radiation wavelength of 1.064 μm the range of nonlinear phase variation $B = 0.5–3$ rad can be realised with the pulses possessing the energy $\varepsilon_p = 0.2–3$ J and duration $t_p = 10$ ps to 4 ns. The chosen range of parameter p variation corresponds to the average power of laser radiation $P = 0.7–7$ kW (Fig. 6b). Hence, of actual interest is the range 0.2–40 kHz of the pulse repetition rate $f = P/\varepsilon_p$.

6. Conclusions

The system of stationary differential equations is obtained, which describes propagation of laser radiation in the medium with circular and linear birefringence under conditions of cubic nonlinearity. The influence of cubic nonlinearity on the value of non-isolation is studied for modern schemes of Faraday isolator: a traditional scheme and schemes with internal and external compensation of thermally induced polarisation distortions.

It was shown that in all the schemes the increase in the non-isolation γ due to cubic nonlinearity is proportional to the square of the B-integral; at $B > 1$ this increase amounts to an order of magnitude and higher. In the scheme with internal compensation and in the optimised scheme with external compensation at the normalised power of heat release $p = 1$ the increase in B from zero to unity results in the reduction of the degree of isolation from 42 to 27 dB; for the optimised scheme with internal compensation this reduction is from 54 to 38 dB. It was shown that, if at $B = 0$ a scheme exhibits a greater isolation then the isolation remains the best under arisen cubic nonlinearity at any thermal load as well.

The estimates of laser radiation parameters are obtained at which the effect of isolation fall due to the combined action of thermal polarisation effects and cubic nonlinearity should be taken into account in the Faraday isolator with a TGG crystal: the pulse energy is 0.2–3 J, pulse duration is 10 ps to 4 ns, pulse repetition rate is 0.2–40 kHz.

References

1. Khazanov E.A., Kulagin O.V., Yoshida S., Tanner D., Reitze D. *IEEE J. Quantum Electron.*, **35** (8), 1116 (1999).
2. Khazanov E., Andreev N., Babin A., Kiselev A., Palashov O., Reitze D. *J. Opt. Soc. Am. B*, **17** (1), 99 (2000).
3. Khazanov E.A. *Kvantovaya Electron.*, **26**, 59 (1999) [*Quantum Electron.*, **29**, 59 (1999)].
4. Andreev N.F., Katin E.V., Palashov O.V., Potyomkin A.K., Reitze D.H., Sergeev A.M., Khazanov E.A. *Kvantovaya Electron.*, **32**, 91 (2002) [*Quantum Electron.*, **32**, 91 (2002)].
5. Snetkov I., Mukhin I., Palashov O., Khazanov E. *Opt. Express*, **19** (7), 6366 (2011).
6. Vlasov S.N., Kryzhanovskii V.I., Yashin V.E. *Kvantovaya Electron.*, **9**, 14 (1982) [*Sov. J. Quantum Electron.*, **12**, 7 (1982)].
7. Maker P.D., Terhune R.W., Savage C.M. *Phys. Rev. Lett.*, **12**, 507 (1964).
8. Kuzmina M.S., Martyanov M.A., Poteomkin A.K., Khazanov E.A., Shaykin A.A. *Opt. Express*, **19** (22), 21977 (2011).
9. Vlasov S.N., Talanov V.I. *Samofokusirovka voln* (Wave Self-focusing) (Novgorod: IPF RAN, 1997).
10. Khazanov E., Andreev N., Palashov O., Poteomkin A., Sergeev A., Mehl O., Reitze D. *Appl. Opt.*, **41** (3), 483 (2002).
11. Massey G.A. *Appl. Phys. Lett.*, **17** (5), 213 (1970).
12. http://www.mt-berlin.com/frames_cryst/descriptions/faraday.
13. http://www.northropgrumman.com/BusinessVentures/SYNOPTICS/Products/SpecialtyCrystals/Pages/TGG.aspx.
14. Andreev N.F., Babin A.A., Zarubina T.V., Kisilev A.M., Palasov O.V., Khazanov E.A., Shchavelev O.S. *Opt. Zh.*, **67**, 66 (2000).
15. Zarubina T.V., Petrovskii G.T. *Opt. Zh.*, **59**, 48 (1992).
16. Malshakov A.N., Pasmanik G.A., Potemkin A.K. *Appl. Opt.*, **36** (25), 6403 (1997).
17. Speck D.R. *IEEE J. Quantum Electron.*, **17**, 1599 (1981).
18. Bunkenberg J., Boles J., Brown D.C., Eastman J., Hoose J., Hopkins R., Iwan L., Jacobs S.D., Kelly J.H., Kumpan S., Letzring S., Lonobile D., Lund L.D., Mourou G., Refermat S., Seka W., Soures J.M., Ken W. *IEEE J. Quantum Electron.*, **17**, 1620 (1981).
19. Bespalov V.I., Talanov V.I. *Pis'ma Zh. Eksp. Teor. Fiz.*, **3**, 471 (1966).
20. Ivanov I., Bulkanov A., Khazanov E., Mukhin I.B., Palashov O.V., Tsvetkov V., Popov P. *Abstr. Conf. CLEO /EUROPE-EQEC 2009* (Munich, Germany, 2009).
21. Guenther K.H., Humpherys T.W., Balmer J., Bettis J.R., Casparis E., Ebert J., Eichner M., Guenther A.H., Kiesel E., Kuehnel R., Milam D., Ryseck W., Seitel S.C., Stewart A.F., Weber H., Weber H.P., Wirtenson G.R., Wood R.M. *Appl. Opt.*, **23** (21), 3743 (1984).
22. Rainer F., Lowdermilk W.H., Milam D. *Opt. Eng.*, **22**, 431 (1983).
23. Amosov A.V., Baranov V.S., Gerasimov S.Yu., Morozov N.V., Sergeev P.B., Stepanchuk V.N. *Kvantovaya Electron.*, **21**, 329 (1994) [*Quantum Electron.*, **24**, 307 (1994)].